

The search for a Hamiltonian whose Energy Spectrum coincides with the Riemann Zeta Zeroes

Raymond Aschheim,* Carlos Castro Perelman†, Klee Irwin‡
Quantum Gravity Research, Topanga, CA. 90290 USA

August 2016

Abstract

Inspired by the Hilbert-Polya proposal to prove the Riemann Hypothesis we have studied the Schroedinger QM equation involving a highly non-trivial potential, and whose self-adjoint Hamiltonian operator has for its energy spectrum one which approaches the imaginary parts of the zeta zeroes only in the *asymptotic* (very large N) region. The ordinates λ_n are the positive imaginary parts of the nontrivial zeta zeros in the critical line : $s_n = \frac{1}{2} + i\lambda_n$. The latter results are consistent with the validity of the Bohr-Sommerfeld semi-classical quantization condition. It is shown how one may modify the parameters which define the potential, and fine tune its values, such that the energy spectrum of the (modified) Hamiltonian matches not only the first two zeroes but the other consecutive zeroes. The highly non-trivial functional form of the potential is found via the Bohr-Sommerfeld quantization formula using the full-fledged Riemann-von Mangoldt counting formula (*without* any truncations) for the number $N(E)$ of zeroes in the critical strip with imaginary part greater than 0 and less than or equal to E .

Keywords: Hilbert-Polya conjecture, Quantum Mechanics, Riemann Hypothesis, Quasicrystals.

1 Introduction

Riemann's outstanding hypothesis [1] that the non-trivial complex zeroes of the zeta-function $\zeta(s)$ must be of the form $s_n = 1/2 \pm i\lambda_n$, is one of most important

*raymond@quantumgravityresearch.org

†perelmanc@hotmail.com

‡klee@quantumgravityresearch.org

open problems in pure mathematics. The zeta-function has a relation with the number of prime numbers less than a given quantity and the zeroes of zeta are deeply connected with the distribution of primes [1]. References [2] are devoted to the mathematical properties of the zeta-function.

The RH (Riemann Hypothesis) has also been studied from the point of view of mathematics and physics by [12], [22], [6], [11], [23], [24], [8], [14], [26], [28], [30] among many others. We refer to the website devoted to the interplay of Number Theory and Physics [20] for an extensive list of articles related to the RH.

A novel physical interpretation of the location of the nontrivial Riemann zeta zeroes which corresponds to the presence of tachyonic-resonances/tachyonic-condensates in bosonic string theory was found in [27] : if there were zeroes outside the critical line violating the RH these zeroes do not correspond to any poles of the string scattering amplitude.

The spectral properties of the λ_n 's are associated with the random statistical fluctuations of the energy levels (quantum chaos) of a classical chaotic system [6]. Montgomery [25] has shown that the two-level correlation function of the distribution of the λ_n 's coincides with the expression obtained by Dyson with the help of Random Matrices corresponding to a Gaussian unitary ensemble.

Extending the results by [28], [29], we were able to construct one-dimensional operators $H_A = D_2 D_1$ and $H_B = D_1 D_2$ in [26] comprised of logarithmic derivatives ($d/dlnt$) and potential terms $V(t)$ involving the Gauss-Jacobi theta series. The Hamiltonians $H_A = D_2 D_1$ and $H_B = D_1 D_2$ had a continuous family of eigenfunctions $\Psi_s(t) = t^{-s+k} e^{V(t)}$ with s being complex-valued and k real such that

$$H_A \Psi_s(t) = s(1-s)\Psi_s(t). \quad H_B \Psi_s\left(\frac{1}{t}\right) = s(1-s)\Psi_s\left(\frac{1}{t}\right). \quad (1.1)$$

Due to the relation $\Psi_s(1/t) = \Psi_{1-s}(t)$ which was based on the modular properties of the Gauss-Jacobi series we were able to show that the eigenvalues $E_s = s(1-s)$ are *real* so that $s = \text{real}$ (location of the trivial zeroes), and/or $s = \frac{1}{2} \pm i\lambda$ (critical line). Furthermore, we showed that the orthogonality conditions

$$\langle \Psi_{\frac{1}{2}+2m}(t) | \Psi_{s_n}(t) \rangle = 0 \Leftrightarrow \zeta(s_n) = 0; \quad s_n = \frac{1}{2} \pm i\lambda_n, \quad m = 1, 2, 3, \dots \quad (1.3)$$

were consistent with the Riemann Hypothesis.

As described by [15], there is considerable circumstantial evidence for the existence of a spectral interpretation of the Riemann zeta zeros [6], [7]. There is a scattering theory interpretation of the Riemann zeta zeros arising from work of [9] concerning the Laplacian acting on the modular surface. Lagarias observed in [10] that there is a natural candidate for a Hilbert-Polya operator, using the framework of the de Branges Hilbert spaces of entire functions, provided that the Riemann hypothesis holds. This interpretation leads to a possible connection with Schroedinger operators on a half-line. Lagarias [15] studied the

Schroedinger Operator with a Morse (exponential) potential on the right half-line and obtained information on the location of zeros of the Whittaker function $W_{\kappa,\mu}(x)$ for fixed real parameters κ, x with $x > 0$, viewed as an entire function of the complex variable μ . In this case all zeroes lie on the imaginary axis, with the possible exception, if $\kappa > 0$. The Whittaker functions and the right half-line are essential ingredients in this present work.

We shall explore further the Hilbert-Polya proposal [3] to generate the zeros in the critical line by constructing an operator $\frac{1}{2} + i\mathcal{H}$ (\mathcal{H} is a self-adjoint operator with *real* eigenvalues) whose spectrum is given by the nontrivial zeta zeroes $s_n = \frac{1}{2} + i\lambda_n$ in the critical line. We should note that the operator $\frac{1}{2} + i\mathcal{H}$ does *not* capture zeros off the critical line in case the Riemann Hypothesis is false. Meyer [8] gave an unconditional formulation of an operator on a more general Banach space whose eigenvalues detect all zeta zeros, including those that are off the critical line if the Riemann hypothesis fails.

The self-adjoint operator \mathcal{H} described here corresponds to the Hamiltonian associated with the Schroedinger QM equation involving a highly non-trivial (fragmented, “fractal” like) see-saw aperiodic potential. In [26] we studied a modified Dirac operator involving a potential related to the number counting function of zeta zeroes and left the Schroedinger operator case for a future project that we undertake in this work. The functional form of the potential is found in section 2 via the Bohr-Sommerfeld quantization formula using the full-fledged Riemann-von Mangoldt counting formula (*without* truncations) for the number $N(E)$ of zeroes in the critical strip with imaginary part greater than 0 and less than or equal to E .

The sought-after single-valued potential is given by a saw potential comprised of an infinite number of finite size tree-like branches. Because it is very difficult to derive the analytical expressions for each one of these branches, in section 3 we *approximate* these infinite branches of the saw potential by a hierarchy of branches whose analytical expressions are of the form $V_k = (M_k x + N_k)^{-2} + \lambda_k$ and which allows to solve exactly the Schroedinger equation in each one of the infinite number of intervals associated with the (approximate) potential branches.

In the first interval ($n = 1$) the wave function is given in terms of Bessel functions, while the wave functions in the following intervals ($n = 2, 3, \dots$) are $\Psi_n(x, E) = a_{n,E} \phi_n(x, E) + b_{n,E} \chi(x, E)$. The numerical amplitude coefficients $a_{n,E}, b_{n,E}$ are energy-dependent and $\phi_n(x, E), \chi_n(x, E)$ are given in terms of the Whittaker functions (which can also be rewritten in terms of modified Bessel functions).

If one matches the values of the wave functions and their derivatives at the boundaries of the intervals, and imposes a relationship among the numerical coefficients of the form $a_{N,E} = 0$, in order to have a vanishing wave function at $x = \infty$, one obtains a discrete energy spectrum that approaches the zeta zeroes only in the *asymptotic* (very large N) region. The latter results are consistent with the validity of the Bohr-Sommerfeld semi-classical quantization condition.

On the other hand, we find that when the energy spectrum $E_n = \lambda_n, n = 2, 3, \dots$, coincides *exactly* with the positive imaginary parts of the nontrivial zeta zeroes in the critical line (except for the first one λ_1), it leads to $a_{n,\lambda_n} =$

∞ ; $b_{n,\lambda_n} = 0$, which does not mean that the wave functions collapse to zero or blow up (as we shall show), and to $a_{n,\lambda_m} \neq 0$; $b_{n,\lambda_m} \neq 0$ when $m \neq n$. It is shown at the end of section **3** how one may *modify* the parameters which define the potential, and fine tune its values, such that the energy spectrum of the (modified) Hamiltonian matches not only the first two zeroes but the other consecutive zeroes. After the concluding remarks on quasicrystals we display *many* figures and a table with numerical values to support our results.

2 Riemann Hypothesis and Bohr-Sommerfeld Quantization

Inspired by the work of [4], [5], we begin with the Schroedinger equation

$$\left\{ -\frac{\hbar^2}{2m} \frac{\partial^2}{\partial x^2} + V(x) \right\} \Psi = E \Psi; \quad \hbar^2 = 2m = 1. \quad (2.1)$$

with the provision that the potential is symmetric $V(-x) = V(x)$. We shall fix the physical units so that $\hbar = 2m = 1 \Rightarrow p = \sqrt{E - V}$, and write the Bohr-Sommerfeld quantization condition $\oint p dx = 2\pi(n + \frac{1}{2})\hbar$ as follows

$$\frac{2}{\pi} \int_{-\infty}^{x_E} \sqrt{E - V} dx = \frac{2}{\pi} \int_{V_0}^E \sqrt{E - V} \frac{dx}{dV} dV = (N(E) - N(V_0)) + \frac{1}{2}. \quad (2.2)$$

we shall see below that $V_0 = V(x = \infty) = E_1$ and why the cycle path begins at $-x_E$, then it goes to $-\infty \rightarrow \infty \rightarrow x_E$ and back. The choice of the \pm signs under the square root $\pm\sqrt{E - V}$ is dictated by the signs of dx/dV in each interval. For example, $dx/dV < 0$ in the $\int_{-\infty}^{x_E}$ integration so one must choose the minus sign $-\sqrt{E - V}$ in order to retrieve a positive number. Eq-(2.2) is $\frac{1}{4}$ of the full cycle of the integral $\oint p dx$ in the Bohr-Sommerfeld formula.

A differentiation of eq-(2.2) w.r.t to E using the most general Leibniz formula for differentiation of a definite integral when the upper $b(E)$ and lower $a(E)$ limits are functions of a parameter E :

$$\begin{aligned} \frac{d}{dE} \int_{a(E)}^{b(E)} f(V; E) dV &= \int_{a(E)}^{b(E)} \left(\frac{\partial f(V; E)}{\partial E} \right) dV + \\ f(V = b(E); E) \left(\frac{d b(E)}{dE} \right) &- f(V = a(E); E) \left(\frac{d a(E)}{dE} \right). \end{aligned} \quad (2.3)$$

leads to

$$\frac{2}{\pi} \frac{d}{dE} \int_{V_0}^E \sqrt{E - V} \frac{dx}{dV} dV = \frac{1}{\pi} \int_{V_0}^E \frac{1}{\sqrt{E - V}} \frac{dx}{dV} dV = \frac{dN(E)}{dE} \quad (2.4)$$

if dx/dV is *not* singular at $V = E$. The above equation belongs to the family of Abel's integral equations corresponding to $\alpha = \frac{1}{2}$ and associated with the unknown function $f(V) \equiv (dx/dV)$

$$\frac{1}{\sqrt{\pi}} \mathcal{J}^{1/2} \left[\frac{dx}{dV} \right] = \frac{1}{\sqrt{\pi}} \frac{1}{\Gamma(1/2)} \int_{V_0}^E \frac{(dx/dV)}{(E-V)^{1/2}} dV = \frac{dN(E)}{dE} \quad (2.5)$$

Abel's integral equation is basically the action of a fractional derivative operator \mathcal{J}^α [32], for the particular value $\alpha = \frac{1}{2}$, on the unknown function $f(V) = (dx/dV)$. Inverting the action of the fractional derivative operator (fractional anti-derivative) yields the solution for

$$\frac{dx}{dV} = \sqrt{\pi} \frac{1}{\Gamma(1/2)} \frac{d}{dV} \int_{V_0}^V \frac{dN(E)}{dE} \frac{1}{(V-E)^{1/2}} dE. \quad (2.6)$$

where the average level counting $\mathcal{N}(E)$ is the Riemann-von Mangoldt formula given below¹. Hence, one has the solution

$$x(V) - x(V_0) = \sqrt{\pi} \frac{1}{\Gamma(1/2)} \int_{V_0}^V \frac{dN(E)}{dE} \frac{1}{(V-E)^{1/2}} dE \quad (2.7)$$

Let us write the functional form for $\mathcal{N}(E)$ to be given by the Riemann-von Mangoldt formula which is valid for $E \geq 1$

$$\mathcal{N}_{RvM}(E) = \frac{E}{2\pi} \left[\log\left(\frac{E}{2\pi}\right) - 1 \right] + \frac{7}{8} + \frac{1}{\pi} \arg \left[\zeta\left(\frac{1}{2} + iE\right) \right] + \frac{1}{\pi} \Delta(E). \quad (2.8)$$

where the (infinitely many times) strongly *oscillating* function is given by the argument of the zeta function evaluated in the critical line

$$S(E) = \frac{1}{\pi} \arg \left[\zeta\left(\frac{1}{2} + iE\right) \right] = \lim_{\epsilon \rightarrow 0} \frac{1}{\pi} \text{Im} \log \left[\zeta\left(\frac{1}{2} + iE + \epsilon\right) \right]. \quad (2.9)$$

the argument of $\zeta(\frac{1}{2} + iE)$ is obtained by the continuous extension of $\arg \zeta(s)$ along the broken line starting at the point $s = 2 + i0$ and then going to the point $s = 2 + iE$ and then to $s = \frac{1}{2} + iE$. If E coincides with the imaginary part of a zeta zero, then

$$S(E_n) = \lim_{\epsilon \rightarrow 0} \frac{1}{2} [S(E_n + \epsilon) + S(E_n - \epsilon)]. \quad (2.10)$$

An extensive analysis of the behaviour of $S(E)$ can be found in [31]. In particular the property that $S(E)$ is a piecewise smooth function with *discontinuities* at the ordinates E_n of the complex zeroes of $\zeta(s_n = \frac{1}{2} + iE_n) = 0$. When E

¹We will show that we can use the solutions to Abel's integral equation despite that $N(E)$ turns out to be discontinuous and non-differentiable at a discrete number of points $E = E_n = \lambda_n$

passes through a point of discontinuity, E_n , the function $S(E)$ makes a jump equal to the sum of multiplicities of the zeta zeroes at that point. The zeros found so far in the critical line are simple [36]. In every interval of continuity (E, E') , where $E_n < E < E' < E_{n+1}$, $S(E)$ is monotonically decreasing with derivatives given by

$$S'(E) = -\frac{1}{2\pi} \log\left(\frac{E}{2\pi}\right) + \mathcal{O}(E^{-2}); \quad S''(E) = -\frac{1}{2\pi E} + \mathcal{O}(E^{-3}). \quad (2.11)$$

The most salient feature of these properties is that the derivative $S'(E)$ blows up at the location of the zeta zeroes E_n due the discontinuity (jump) of $S(E)$ at E_n . Also, the strongly oscillatory behaviour of $S(E)$ forces the potential $V(x)$ to be a multi-valued function of x .

The expression for $\Delta(E)$ is [31]

$$\Delta(E) = \frac{E}{4} \log\left(1 + \frac{1}{4E^2}\right) + \frac{1}{4} \arctan\left(\frac{1}{2E}\right) - \frac{E}{2} \int_0^\infty \frac{\rho(u) du}{(u + 1/4)^2 + (E/2)^2}. \quad (2.12)$$

with $\rho(u) = \frac{1}{2} - \{u\}$, where $\{u\}$ is the fractional part of u and which can be written as $u - [u]$, where $[u]$ is the integer part of u . In this way one can perform the integral involving $[u]$ in the numerator by partitioning the $[0, \infty]$ interval in intervals of unit length : $[0, 1], [1, 2], [2, 3], \dots, [n, n+1], \dots$

The graph of the $N(E)$ level counting function is displayed in fig-1. The derivative $\frac{dN(E)}{dE}$ is given by a Dirac-comb of the form

$$\frac{dN(E)}{dE} = \sum_{n=1}^{\infty} \delta(E - E_n) \quad (2.13)$$

After taking the derivative of the Bohr-Sommerfeld quantization formula eq-(2.2), upon using the Leibniz rule (2.3) and the solution eq-(2.6) to Abel's integral equation, leads to

$$\begin{aligned} \frac{dx}{dV} &= \sqrt{\pi} \frac{1}{\Gamma(1/2)} \frac{d}{dV} \int_{V_0}^V \frac{dN(E)}{dE} \frac{1}{(V-E)^{1/2}} dE = \\ &= -\frac{1}{2} \int_{V_0}^V \left(\sum_{E_n < E} \delta(E - E_n) \frac{1}{(V-E)^{3/2}} \right) dE + \sum_{E_n < V} \delta(V - E_n) \frac{1}{(V-V)^{1/2}} = \\ &= -\frac{1}{2} \sum_{E_n < V} \frac{1}{(V-E_n)^{3/2}} + \sum_{E_n < V} \delta(V - E_n) \frac{1}{(V-V)^{1/2}} \quad (2.14) \end{aligned}$$

The last terms $\delta(V - E_n) \frac{1}{(V-V)^{1/2}}$ are 0 when $E_n \neq V$ (due to the fact that $\delta(V - E_n) = 0$ goes to zero faster than the denominator), and are equal to ∞ when $E_n = V$. Consequently one learns that dx/dV has poles only at the locations $V = E_n$. If we take $E > E_n$ for all values of n , then dx/dV will be

finite at $V = E$ and such that eq-(2.4) will remain *unmodified* after using the generalized Leibniz rule.

From eq- (2.14) we can also deduce the exact expression for $x = x(V)$

$$x(V) = \sqrt{\pi} \frac{1}{\Gamma(1/2)} \int_{V_0}^V \frac{d\mathcal{N}(E)}{dE} \frac{1}{(V-E)^{1/2}} dE = \sum_{E_n < V} \frac{1}{(V-E_n)^{1/2}} \quad (2.15)$$

from which one can infer that $V_0 = E_1 \Rightarrow x(V_0) = x(E_1) = \infty$ so that the lowest point V_0 is consistent with the following expression

$$x(V) - x(V_0) = \sum_{E_n < V} \frac{1}{(V-E_n)^{1/2}} - \frac{1}{(V_0-E_1)^{1/2}} \quad (2.16)$$

One learns that there are many different branches of the function $x(V)$. In the V -interval $[E_1, E_2]$ one has

$$x(V) = \frac{1}{(V-E_1)^{1/2}} \Rightarrow V_1(x) = \frac{1}{x^2} + E_1 \quad (2.17a)$$

where the domain of $V_1(x)$ is

$$x \in (-\infty, -x_1] \cup [x_1, \infty), \quad x_1 = \frac{1}{\sqrt{E_2 - E_1}} \quad (2.17b)$$

In the V -interval $[E_2, E_3]$ one has

$$x(V) = \frac{1}{(V-E_1)^{1/2}} + \frac{1}{(V-E_2)^{1/2}} \quad (2.18)$$

and so forth, in the V -interval $[E_n, E_{n+1}]$ one has

$$x(V) = \frac{1}{(V-E_1)^{1/2}} + \frac{1}{(V-E_2)^{1/2}} + \dots + \frac{1}{(V-E_n)^{1/2}} \quad (2.19)$$

Inverting these functions is a highly nontrivial task. For example, inverting (2.18) to determine $V(x)$ requires solving a polynomial equation of *quartic* degree in V . Despite that $\frac{dx}{dV}$ *diverges* due to the presence of the poles whenever $V = E_n$, we shall show that the integral (2.2) is finite due to an explicit cancellation of these poles in the Bohr-Sommerfeld formula. Because there are many different branches of the function $x(V)$ one has to *split* up the V -integral (2.2) into different V -intervals (beginning with $V_0 = E_1$) as follows

$$\begin{aligned} \frac{2}{\pi} \int_{V_0}^E \sqrt{E-V} \frac{dx}{dV} dV &= \frac{2}{\pi} \int_{E_1}^{E_1} \sqrt{E-V} \frac{dx}{dV} dV + \\ \frac{2}{\pi} \int_{E_1}^{E_2} \sqrt{E-V} \left(-\frac{1}{2} \frac{1}{(V-E_1)^{3/2}} + \delta(V-E_1) \frac{1}{(V-V)^{1/2}} \right) dV &+ \end{aligned}$$

$$\begin{aligned}
& \frac{2}{\pi} \int_{E_2}^{E_3} \sqrt{E-V} \left(-\frac{1}{2} \left(\frac{1}{(V-E_1)^{3/2}} + \frac{1}{(V-E_2)^{3/2}} \right) + \delta(V-E_2) \frac{1}{(V-V)^{1/2}} \right) dV + \dots \\
& + \frac{2}{\pi} \int_{E_N}^E \sqrt{E-V} \left(-\frac{1}{2} \right) \left(\frac{1}{(V-E_1)^{3/2}} + \frac{1}{(V-E_2)^{3/2}} + \dots + \frac{1}{(V-E_N)^{3/2}} \right) dV + \\
& \qquad \qquad \qquad \frac{2}{\pi} \int_{E_N}^E \sqrt{E-V} \delta(V-E_N) \frac{1}{(V-V)^{1/2}} dV \qquad (2.20)
\end{aligned}$$

After performing the integrals (2.20) for all values of $n = 1, 2, \dots, N$, with

$$\int \frac{\sqrt{E-V}}{(V-E_n)^{3/2}} dV = 2 \arctan\left(\frac{\sqrt{E-V}}{\sqrt{V-E_n}}\right) - 2 \frac{\sqrt{E-V}}{\sqrt{V-E_n}} \qquad (2.21)$$

one learns the following facts :

(i) There is an *exact* cancellation of *all* the poles

$$-\frac{2}{\pi} \sum_n \frac{(E-E_n)^{1/2}}{(E_n-E_n)^{1/2}} + \frac{2}{\pi} \sum_n \frac{(E-E_n)^{1/2}}{(E_n-E_n)^{1/2}} = 0 \qquad (2.22)$$

(ii) The contribution from the upper limits of the integrals $\int_{E_m}^{E_{m+1}}$ cancel out *most* of the contributions from the lower limits of the integrals of the next interval $\int_{E_{m+1}}^{E_{m+2}}$

(iii) The contribution from the upper limit of the last integral $\int_{E_N}^E$ is identically zero

$$2 \arctan\left(\frac{\sqrt{E-E}}{\sqrt{E-E_N}}\right) - 2 \frac{\sqrt{E-E}}{\sqrt{E-E_N}} = 0 \qquad (2.23)$$

(iv) Leaving for the *net* contribution to the integrals (2.20), when $E > E_n$ for all $n = 1, 2, \dots, N$, the following sum

$$\frac{2}{\pi} \sum_{n=1}^{n=N} \arctan\left(\frac{\sqrt{E-E_n}}{\sqrt{E_n-E_n}}\right) = \frac{2}{\pi} \frac{\pi}{2} N = N; \quad E > E_n \qquad (2.24)$$

where we have set $N(V_0) = N(E_1) = \frac{1}{2}$ in eq-(2.2) so that $-N(V_0) + \frac{1}{2} = 0$. Choosing $N(V_0) = N(E_1) = \frac{1}{2}$ is tantamount of taking the *average* between 0 and 1 which are the number of (positive) energy levels less than or equal to E_1 , respectively.

Therefore, we can safely conclude that the exact expressions for $N(E)$ and $\frac{dN(E)}{dE}$ to be used in eqs-(2.2, 2.14) are indeed consistent with the solutions to the Abel integral equation (2.6) for the parameter $\alpha = 1/2$. This consistency occurs even if $N(E)$ is discontinuous at the location of each energy level E_n , and the derivatives $\frac{dN(E)}{dE}$ are given by the Dirac-comb expression (2.13); i.e. the derivatives are singular at E_n .

3 The Construction of a Single-Valued Potential

Self-Adjoint Hamiltonian

In order to construct a Hamiltonian operator which is self-adjoint one also needs to specify the domain in the x -axis over which the Hamiltonian is defined. In particular the eigenfunctions must have compact support and be square-integrable to ensure that inner products are well-defined. An operator \mathbf{A} is defined not only by its action, but also by its *domain* \mathcal{D}_A , the space of (square integrable) functions on which it acts [33]. If $\mathbf{A} = \mathbf{A}^\dagger$ and $\mathcal{D}_{A^\dagger} = \mathcal{D}_A$ the operator is said to be self-adjoint [33].

We note that the first branch of the potential is *not* defined in the interval $[-x_1, x_1]$ with $x_1 = \frac{1}{\sqrt{E_2 - E_1}}$. In order to solve this problem we shall erect an *infinite* potential barrier at $\pm x_1$ so that the wave-functions $\Psi(x)$ evaluated *inside* the interval $[-x_1, x_1]$ are *zero* and the quantum particle never reaches the interior region of the interval $[-x_1, x_1]$. The Hamiltonian is self adjoint in this case because

$$\begin{aligned} \int_{-\infty}^{\infty} \Psi^* \frac{d^2\Psi}{dx^2} dx &= \int_{-\infty}^{-x_1} \Psi^* \frac{d^2\Psi}{dx^2} dx + \int_{-x_1}^{x_1} \Psi^* \frac{d^2\Psi}{dx^2} dx + \int_{x_1}^{\infty} \Psi^* \frac{d^2\Psi}{dx^2} dx = \\ &= \int_{-\infty}^{-x_1} \Psi^* \frac{d^2\Psi}{dx^2} dx + \int_{x_1}^{\infty} \Psi^* \frac{d^2\Psi}{dx^2} dx \end{aligned} \quad (3.1)$$

Performing an integration by parts twice and taking into account that $\Psi(x), \Psi^*(x)$ *vanish* at $x = \pm\infty$ and $x = \pm x_1$, the integral (3.1) becomes

$$\int_{-\infty}^{-x_1} \frac{d^2\Psi^*}{dx^2} \Psi dx + \int_{x_1}^{\infty} \frac{d^2\Psi^*}{dx^2} \Psi dx = \int_{-\infty}^{\infty} \frac{d^2\Psi^*}{dx^2} \Psi dx \quad (3.2)$$

Hence, the equality of eq-(3.1) and eq-(3.2) reveals that the Hamiltonian in eq-(2.1) is self adjoint. Similar conclusions apply when one has a potential defined on a half-line $[x_1, \infty)$ if the wave functions obey the boundary conditions $\Psi(x_1) = 0; (d\Psi/dx)(x_1) \neq \infty$ and $\Psi(x) \rightarrow 0, (d\Psi(x)/dx) \rightarrow 0$ as $x \rightarrow \infty$.

The remaining step before solving the Schroedinger equation is to extract a **single**-valued potential comprised of finite tree-like branches that are defined over a sequence of finite intervals in the x -axis. See figures. The first branch of the potential was already defined above in eqs-(2.17a, 2.17b). The second branch of the potential is defined in $(-\infty, -x_2] \cup [x_2, \infty)$ where

$$x_2 = \frac{1}{\sqrt{E_3 - E_1}} + \frac{1}{\sqrt{E_3 - E_2}} \quad (3.3)$$

The third branch of the potential is defined in the interval $(-\infty, -x_3] \cup [x_3, \infty)$ where

$$x_3 = \frac{1}{\sqrt{E_4 - E_1}} + \frac{1}{\sqrt{E_4 - E_2}} + \frac{1}{\sqrt{E_4 - E_3}} \quad (3.4)$$

and so forth. In order to extract a **single**-valued potential we may select the appropriate **finite** tree-branches as follows :

In the interval $[x_1, x_2]$ we choose the **first** branch of the saw potential and label it by $V_1(x)$ such that $V_1(x_1) = E_2 = \lambda_2$. In the interval $[x_2, x_3]$ we choose the **second** branch of the saw potential and label it by $V_2(x)$ such that $V_2(x_2) = E_3 = \lambda_3$. In the interval $[x_3, x_4]$ we choose the **third** branch of the saw potential and label it by $V_3(x)$, such that $V_3(x_3) = E_4 = \lambda_4$, and so forth. Most of the coordinates of the points x_n are in sequential order *except* in some cases where $x_m < x_n$ despite $m > n$. In this case we have to introduce a *reordering*. If, and only if, there are very exceptional cases such that $x_m = x_n$ one will encounter a problem in constructing a single-valued potential for all $x \geq x_1$. We believe that there are no cases such that $x_m = x_n$.

Having extracted the single-valued saw potential in this fashion, with an infinite potential barrier at x_1 , we proceed to solve the Schroedinger equation in each interval region subject to the conditions that the values of Ψ and $(d\Psi/dx)$ must *match* at the *boundaries* of all of these infinite number of intervals. This is a consequence of the conservation of probability for quantum stationary states. This is how one may find the spectrum of energy levels (bound states) associated with the single-valued saw potential. It is then when one can ascertain whether or not one recovers the positive imaginary parts of the non-trivial zeta zeros in the critical line for the physical energy spectrum. Since the saw potential can be seen as a hierarchy of *deformed* potential wells, this procedure (however daunting) is no different than finding the bound states of a periodic potential well [21] leading to energy bands and gaps.

Approximate Potentials and Solutions in terms of Whittaker Functions

Let us take the potential in the first region to be given by the exact expression $V_1 = \frac{1}{x^2} + \lambda_1$ ($E_1 = \lambda_1$) while the potential in the other intervals are given by the *approximate* version

$$V_k^{approx}(x) = \frac{1}{(M_k x + N_k)^2} + \lambda_k, \quad E_k = \lambda_k, \quad k = 2, 3, \dots \quad (3.5)$$

It is well known to the experts that the Quantum Mechanics of the $1/x^2$ potential on $0 < x < \infty$ is very subtle with all sorts of paradoxes whose solutions requires a sophisticated theoretical machinery [33]. For this reason, we just limit ourselves to solving the Schroedinger equation.

Setting aside the *reordering* of x_k for the moment, the numerical coefficients M_k, N_k are obtained by imposing the following conditions

$$\begin{aligned} V_k^{approx}(x = x_k) &= E_{k+1} = \lambda_{k+1} \\ V_k^{approx}(x = x_{k+1}) &= V_k(x = x_{k+1}) > E_k = \lambda_k \end{aligned} \quad (3.6)$$

In Table-1 we display the first six values of M_k, N_k . The solutions to the Schroedinger equation in the first region are given in terms of Bessel functions

$$\Psi_1(x; E) = a_1 \sqrt{x} J_{\sqrt{5}/2}[\sqrt{E - E_1} x] + b_1 \sqrt{x} Y_{\sqrt{5}/2}[\sqrt{E - E_1} x] \quad (3.7)$$

while the solutions in the other regions are given in terms of the Whittaker functions after performing the change of variables

$$z = \frac{M_k x + N_k}{M_k^2} (2M_k \sqrt{E_k - E}), \quad k = 2, 3, \dots, \quad (3.8)$$

which convert the Schroedinger equation into the Whittaker differential equation

$$\frac{d^2 F}{dz^2} + \left(-\frac{1}{4} + \frac{\frac{1}{4} - \mu^2}{z^2} \right) F = 0 \quad (3.9)$$

for the particular value of the parameter $\kappa = 0$. Thus, the general solutions to the Schroedinger equation in the regions beyond the first interval are given by linear combinations of two functions related to the Kummer functions [15]

$$\phi_k(x, E) = M_{0, -\sqrt{\frac{M_k^2 + 4}{2M_k}}} \left(\frac{2\sqrt{E_k - E} (xM_k + N_k)}{M_k} \right) \quad (3.10)$$

$$\chi_k(x, E) = W_{0, -\sqrt{\frac{M_k^2 + 4}{2M_k}}} \left(\frac{2\sqrt{E_k - E} (xM_k + N_k)}{M_k} \right) \quad (3.11)$$

of the form

$$\Psi_k(x, E) = a_k \phi_k(x, E) + b_k \chi_k(x, E), \quad k = 2, 3, \dots, \quad (3.12)$$

In the most general case $\kappa \neq 0$ the differential equation is [15], [16]

$$\frac{d^2 F}{dz^2} + \left(-\frac{1}{4} + \frac{\kappa}{z} + \frac{\frac{1}{4} - \mu^2}{z^2} \right) F = 0 \quad (3.13)$$

the two independent solutions are

$$M_{\kappa, \mu}(z) = e^{-\frac{\kappa}{z}} z^{\mu + \frac{1}{2}} {}_1F_1 \left(-\kappa + \mu + \frac{1}{2}; 2\mu + 1; z \right) \quad (3.14)$$

where ${}_1F_1(-\kappa + \mu + \frac{1}{2}; 2\mu + 1; z)$ is a confluent hypergeometric function,

$${}_1F_1(a; b; z) = \sum_{k=0}^{\infty} \frac{(a)_k}{(b)_k} \frac{z^k}{k!} \quad (3.15a)$$

$$\begin{aligned} (a)_k &= a(a+1)(a+2)\dots(a+k-1); \quad (a)_0 = 1 \\ (b)_k &= b(b+1)(b+2)\dots(b+k-1); \quad (b)_0 = 1 \end{aligned} \quad (3.15b)$$

and

$$W_{\kappa, \mu}(z) = e^{-\frac{\kappa}{z}} z^{\mu + \frac{1}{2}} U \left(-\kappa + \mu + \frac{1}{2}; 2\mu + 1; z \right) \quad (3.16)$$

with

$$U(a, b, z) = \frac{1}{\Gamma(a)} \int_0^\infty dt t^{a-1} (t+1)^{b-a-1} e^{-zt} \quad (3.17)$$

The Whittaker function $W_{\kappa, \mu}(z)$ is specified by the asymptotic property of having rapid *decrease* as $z = x \rightarrow \infty$ along the positive real axis [15]. In terms of the confluent hypergeometric function one has [15], [16]

$$W_{\kappa, \mu}(z) = \frac{\Gamma(-2\mu)}{\Gamma(\frac{1}{2} - \kappa - \mu)} M_{\kappa, \mu}(z) + \frac{\Gamma(2\mu)}{\Gamma(\frac{1}{2} - \kappa + \mu)} M_{\kappa, -\mu}(z) \quad (3.18)$$

from which one can infer that $W_{\kappa, \mu}(z) = W_{\kappa, -\mu}(z)$. All other linearly independent solutions to Whittaker's differential equation increase rapidly (in absolute value) along the positive real axis as $x \rightarrow \infty$. In the following subsections we will have $\kappa = 0$, and $\mu_k = \frac{M_k^2 + 4}{2M_k}$, $k = 2, 3, \dots$ so there will not be any confusion between κ and $k = 2, 3, \dots$.

To finalize this subsection we may add that one could have also expressed the wave function solutions in terms of the modified Bessel functions I_ν, K_ν or the Bessel functions J_ν, Y_ν if one wishes. For instance, the Whittaker functions $M_{0, \mu}(2z), W_{0, \mu}(2z)$ can be rewritten respectively [16] as

$$M_{0, \mu}(2z) = 2^{2\mu + \frac{1}{2}} \Gamma(1 + \mu) \sqrt{z} I_\mu(z); \quad W_{0, \mu}(2z) = \sqrt{\frac{2}{\pi}} \sqrt{z} K_\mu(z) \quad (3.19a)$$

when $\mu \neq$ integer, $I_\mu(z)$ and $I_{-\mu}(z)$ are linearly independent so that $K_\mu(z)$ can be re-expressed as [16]

$$K_\mu(z) = \frac{\pi}{2 \sin(\mu\pi)} (I_{-\mu}(z) - I_\mu(z)) \quad (3.19b)$$

$K_\mu(z)$ tends to zero as $|z| \rightarrow \infty$ in the sector $|\arg z| < \frac{\pi}{2}$ for all values of μ . They also can be rewritten with the Hankel or Bessel functions [17][18][19] as

$$M_{0, \mu}(2z) = (-4i)^\mu \Gamma(\mu + 1) \sqrt{z} J_\mu(iz) \quad (3.19c)$$

$$W_{0, \mu}(2z) = i^{\mu+1} \frac{\sqrt{\pi}}{2} \sqrt{z} H_\mu^{(1)}(iz) = i^{\mu+1} \frac{\sqrt{\pi}}{2} \sqrt{z} (J_\mu(iz) + i Y_\mu(iz)) \quad (3.19d)$$

The Energy spectrum

Before finding the energy spectrum it is required to focus on the wave function in the first interval. From the condition $\Psi_1(x_1, E) = 0$,

$$\Psi_1(x_1, E) = a_{1, E} \sqrt{x_1} J_{\sqrt{5}/2}[\sqrt{E - E_1} x_1] + b_{1, E} \sqrt{x_1} Y_{\sqrt{5}/2}[\sqrt{E - E_1} x_1] = 0 \quad (3.20a)$$

one learns that the ratio $a_{1,E}/b_{1,E}$ is given by

$$\frac{a_{1,E}}{b_{1,E}} = - \frac{Y_{\sqrt{5}/2}[\sqrt{E-E_1} x_1]}{J_{\sqrt{5}/2}[\sqrt{E-E_1} x_1]} \quad (3.20b)$$

and it is an explicit function of the energy E . It is interesting that the order $\sqrt{5}/2$ of the Bessel function is closely related to the Golden mean $(1 + \sqrt{5})/2$. When $E = E_1 = \lambda_1$, the Bessel function $Y_{\sqrt{5}/2}[\sqrt{E-E_1} x_1] \rightarrow Y_{\sqrt{5}/2}(0)$ blows up, so one must have $b_{1,\lambda_1} = 0$. Since the Bessel function $J_{\sqrt{5}/2}(0)$ is finite and nonzero, then a_{1,λ_1} is finite and nonzero.

A similar analysis for the wave functions in the other intervals allows to deduce that when the energy spectrum $E_n = \lambda_n, n = 2, 3, \dots$, coincides *exactly* with the positive imaginary parts of the nontrivial zeta zeroes in the critical line (except for the first one λ_1), it leads to $a_{n,\lambda_n} = \infty$; $b_{n,\lambda_n} = 0$, which does not mean that the wave functions collapse to zero or blow up. This fact simply follows from the behavior of the Whittaker functions at $z = 0$

$$M_{0,-\frac{\sqrt{M_k^2+4}}{2M_k}} \left(\frac{2\sqrt{E_k-E_k}(xM_k+N_k)}{M_k} \right) = 0, \quad E_k = \lambda_k \quad (3.21a)$$

$$W_{0,-\frac{\sqrt{M_k^2+4}}{2M_k}} \left(\frac{2\sqrt{E_k-E_k}(xM_k+N_k)}{M_k} \right) = \infty, \quad E_k = \lambda_k \quad (3.21b)$$

so that $a_{k,\lambda_k} M_{0,-\frac{\sqrt{M_k^2+4}}{2M_k}}(0) = \infty \times 0$; and $b_{k,\lambda_k} W_{0,-\frac{\sqrt{M_k^2+4}}{2M_k}}(0) = 0 \times \infty$. Since the latter products are *undetermined*, the corresponding wave functions are not well defined (in the k -th interval) when the energy E_k coincides with the zeta zero λ_k . Consequently one must find another spectrum associated to well defined wave functions, even if $a_{n,\lambda_m} \neq \infty$; $b_{n,\lambda_m} \neq 0$ when $m \neq n$.

If one matches the values of the wave functions, and their derivatives at the boundaries of the intervals (resulting from conservation of the quantum probability), one can deduce the relationships among the numerical amplitude coefficients. In this case the general recursion relation among the (a_n, b_n) and (a_1, b_1) coefficients is of form

$$\mathbf{C}_n = \mathbf{L}_{n,n-1} \mathbf{L}_{n-1,n-2} \dots \mathbf{L}_{2,1} \mathbf{C}_1 \quad (3.22)$$

where $\mathbf{C}_1, \mathbf{C}_n$ are two column matrices whose two entries are comprised of $(a_1, b_1), (a_n, b_n)$, respectively, and \mathbf{L} 's are the chain of 2×2 matrices that relate the coefficients a_i, b_i in terms of the previous ones a_{i-1}, b_{i-1} . The entries of the chain of matrices \mathbf{L} 's are comprised of products Whittaker functions and their derivatives evaluated at different arguments $M_i x_i + N_i$ associated to the intervals involved. The four entries of the final 2×2 matrix \mathbf{S} resulting from the product of the ladder matrices

$$\mathbf{S} \equiv \mathbf{L}_{n,n-1} \mathbf{L}_{n-1,n-2} \dots \mathbf{L}_{2,1} \quad (3.23)$$

are given by $S_{11}, S_{12}, S_{21}, S_{22}$, respectively. Therefore, the relationships among the numerical amplitude coefficients is

$$a_{n,E} = a_{1,E} \left(S_{11}(E) - S_{12}(E) \frac{J_{\sqrt{5}/2}(\sqrt{E-E_1} x_1)}{Y_{\sqrt{5}/2}(\sqrt{E-E_1} x_1)} \right) \quad (3.24a)$$

$$b_{n,E} = a_{1,E} \left(S_{21}(E) - S_{22}(E) \frac{J_{\sqrt{5}/2}(\sqrt{E-E_1} x_1)}{Y_{\sqrt{5}/2}(\sqrt{E-E_1} x_1)} \right) \quad (3.24b)$$

The above relations (3.24) determine $a_{n,E}, b_{n,E}$ in terms of $a_{1,E}$, and which in turn, is determined by imposing the normalization condition on the wave functions $\int_{x_1}^{\infty} dx \Psi^*(x, E) \Psi(x, E) = 1$ as explained below.

Another discrete energy spectrum can be found leading to well defined wave functions. It is obtained by imposing certain conditions on the values of the numerical coefficients $a_{n,E}, b_{n,E}$ [21]. Because the wave functions $\Psi(x, E)$ must *decrease* fast enough towards 0 as $x \rightarrow \infty$, as required in order to have a self-adjoint Hamiltonian operator on the half-line $[x_1, \infty)$, this will guide us in choosing the right conditions. As mentioned earlier in eq-(3.18), the Whittaker function $W_{\kappa, \mu}(z)$ is specified by the asymptotic property of having rapid *decrease* as $z = x \rightarrow \infty$ along the positive real axis [15].

The simplest procedure would be to modify the saw potential branches in the region $[x_N, \infty)$, for a very large value of N , by choosing

$$V_N(x) = \frac{1}{(M_N x + N_N)^2} + \lambda_N, \quad x \in [x_N, \infty) \quad (3.25)$$

and truncating the coefficient $a_{N,E} = 0$ so that the wave function in the region defined by $[x_N, \infty)$ becomes

$$\Psi_N(x, E) = b_{N,E} \chi_N(x, E) = b_{N,E} W_{0, -\frac{\sqrt{M_N^2+4}}{2M_N}} \left(\frac{2\sqrt{E_N - E}(xM_N + N_N)}{M_N} \right), \quad x \in [x_N, \infty) \quad (3.26)$$

so that $\Psi_N(x, E)$ has a rapid decrease to 0 as $x \rightarrow \infty$. Similar results would follow if one rewrote the solutions in terms of the modified Bessel functions by simple inspection of eqs-(3.18, 3.19a, 3.19b). After truncating $a_{N,E} = 0$ one still has to obey the matching conditions involving the previous interval

$$\Psi_{N-1}(x_N, E) = \Psi_N(x_N, E), \quad \left(\frac{d\Psi_{N-1}(x, E)}{dx} \right)_{(x_N)} = \left(\frac{d\Psi_N(x, E)}{dx} \right)_{(x_N)} \quad (3.27)$$

Hence, after factoring $a_{1,E} \neq 0$ in (3.24a), one arrives finally at the transcendental equation (in the energy) given by

$$a_{N,E} = 0 \Rightarrow S_{11}(E) - S_{12}(E) \frac{J_{\sqrt{5}/2}(\sqrt{E-E_1} x_1)}{Y_{\sqrt{5}/2}(\sqrt{E-E_1} x_1)} = 0 \quad (3.28)$$

the above equation $a_{N,E} = 0$ is called the characteristic equation and whose solutions $E = E'_1, E'_2, \dots, E'_{k(N)}$ yield the discrete energy spectrum. Given N , the number of roots of eq-(3.28) is itself dependent on N and for this reason we label them as $1, 2, \dots, k = k(N)$. We display in some of the figures (figures 7,11,12 at the end of this work) the graphs of the characteristic equation (3.28), and its roots, for some values of N .

Having determined the energy spectrum from eq-(3.28) we insert those energy values into

$$b_{N,E'_k} = a_{1,E'_k} \left(S_{21}(E'_k) - S_{22}(E'_k) \frac{J_{\sqrt{5}/2}(\sqrt{E'_k - E_1} x_1)}{Y_{\sqrt{5}/2}(\sqrt{E'_k - E_1} x_1)} \right) \quad (3.29)$$

and determine the non-vanishing values for $b_{N,E'_1}, b_{N,E'_2}, \dots, b_{N,E'_{k(N)}}$, which in turn, yield the expression for the wave function $\Psi_N(x, E'_k)$ given by eq-(3.26) and corresponding to the energy values $E = E'_k, k = 1, 2, 3, \dots, k(N)$. Eqs-(3.24) yield the other values of a_{n,E'_k}, b_{n,E'_k} for $n < N$, and eq-(3.12) will then determine the wave functions in all the previous intervals to the N -th one. We should note that the (global) wave function $\Psi(x, E'_k)$ still has an explicit dependence on the arbitrary a_{1,E'_k} coefficient. It is then when one can *fix* its value from the normalization condition $\int_{x_1}^{\infty} dx \Psi^*(x, E'_k) \Psi(x, E'_k) = 1$.

Because the wave functions $\Psi(x, E)$ are fixed to *decrease* fast enough towards 0 as $x \rightarrow \infty$, they are normalizable leading to a finite nonzero value for the a_{1,E'_k} coefficients. The wave function $\Psi(x, E'_k)$ is comprised (stitched) of many different pieces from the wave functions in all of the intervals

$$\Psi_1(x, E'_k), \Psi_2(x, E'_k), \Psi_3(x, E'_k), \dots, \Psi_N(x, E'_k) \quad (3.30)$$

This stitching procedure of the saw potential into many different branches, and of $\Psi(x, E'_k)$ into many different pieces, can roughly be thought of a “fractalization” or fragmentation. The discrete energy spectrum will approach the zeta zeroes only in the *asymptotic* region (very large values of N) and which is consistent with the validity of the Bohr-Sommerfeld semi-classical quantization condition. The normalization of the wave functions and the study of their asymptotic properties will be the subject of future investigations.

Infrared Fine-Tuning

To finalize this section we should add that many deformations of the saw potential are possible such that the small eigenvalues of the deformed Hamiltonian coincide with the first zeroes of zeta and without changing the asymptotic energy spectrum. One method described here is based in a judicious scaling of the set of zeroes (which allowed the construction of the saw potential) by a logistic function,

This scaling allows to deform the potential and fit the first zeroes as shown in figure-(8). The infrared part of the spectrum is comprised of the low energy solutions of the characteristic equation eq-(3.28) and leads to values which don't

coincide to the low values of the zeta zeroes. We can still maintain the same functional form (shape) of the potential while *modifying* the values of E_1, E_2, E_3, \dots such that $\hat{E}_k = \hat{\lambda}_k = E_k f(k)$, where $f(k)$ is an interval-dependent scaling factor.

Hence, the modified potential in each interval is now given by

$$\hat{V}_k(x) = \frac{1}{(\hat{M}_k x + \hat{N}_k)^2} + \hat{\lambda}_k, \quad \hat{\lambda}_k = E_k f(k), \quad k = 1, 2, 3, \dots \quad (3.31)$$

Any function $f(k)$ converging to 1 as $k \rightarrow \infty$ can be used as the scaling function. For example, the following logistic function (where γ is negative)

$$f(x) = \frac{\alpha e^{\gamma x} + 1}{\beta e^{\gamma x} + 1} \quad (3.32)$$

To facilitate (speed up) the computations, it is convenient to choose a new basis for the wavefunctions. Hence, eqs-(3.7), (3.10), (3.11) and (3.12) are now replaced by

$$\begin{aligned} \Psi_k(x; E) &= c_k \sqrt{x + \frac{N_k}{M_k}} J_{\frac{\sqrt{M_k^2+4}}{2M_k}} \left[\left(x + \frac{N_k}{M_k}\right) \sqrt{E - E_k} \right] \\ &+ d_k \sqrt{x + \frac{N_k}{M_k}} Y_{\frac{\sqrt{M_k^2+4}}{2M_k}} \left[\left(x + \frac{N_k}{M_k}\right) \sqrt{E - E_k} \right] \end{aligned} \quad (3.33)$$

For $k = 1$ one recovers eq-(3.7) with $M_1 = 1$ and $N_1 = 0$.

The wave function solutions associated to the the deformed potential (3.31) are now given by

$$\begin{aligned} \hat{\Psi}_k(x, E) &= c_k \sqrt{x + \frac{\hat{N}_k}{\hat{M}_k}} J_{\frac{\sqrt{\hat{M}_k^2+4}}{2\hat{M}_k}} \left[\left(x + \frac{\hat{N}_k}{\hat{M}_k}\right) \sqrt{E - \hat{\lambda}_k} \right] \\ &+ d_k \sqrt{x + \frac{\hat{N}_k}{\hat{M}_k}} Y_{\frac{\sqrt{\hat{M}_k^2+4}}{2\hat{M}_k}} \left[\left(x + \frac{\hat{N}_k}{\hat{M}_k}\right) \sqrt{E - \hat{\lambda}_k} \right] \end{aligned} \quad (3.34)$$

From (3.19c, 3.19d), we get $c_{n,E} + id_{n,E} = (-4i)^\mu \Gamma(1 + \mu) a_{n,E}$ with $\mu = \frac{\sqrt{M_n^2+4}}{2M_n}$. Due to the *change* of basis (3.33, 3.34), the characteristic equation (3.28) $a_{n,E} = 0$ is now *replaced* by $c_{n,E} + id_{n,E} = 0$. To fine tune its solutions, in order to match the low values of the first zeta zeros, we may choose the interval number $n = 11$ and fine tune the values of α, β, γ in eq-(3.32), starting at $\alpha = 500, \beta = 1000, \gamma = -1$, by solving the equation numerically so that the first two zeroes of $(c_n + id_n)(E)$ (for $n = 11$) converge to $E = E_1 = \lambda_1$ and $E = E_2 = \lambda_2$. The fine tuning is achieved by alternatively changing the value of $\alpha, \gamma, \beta, \gamma, \alpha \dots$ until convergence. See figure-(8). In figures-(9,10) we display the graphs of the wave functions for $n = 11$ intervals and corresponding to E_1, E_2 , respectively.

Now it remains to fine tune the parameters of the modified potential, for larger and larger values of the interval number n , in order for the solutions $c_{n,E} + id_{n,E} = 0$ to match not only the first two zeroes but the other consecutive zeroes. Consequently we have to repeat the same procedure for the next zeroes. As one increases the values of the interval-number n (towards infinity) the parameters of the scaling function (3.32) α, β, γ can be fine tuned such that the spectrum converges to the zeta zeroes.

4 Concluding Remarks

The Bohr-Sommerfeld formula, in conjunction with the full-fledged Riemann-von Mangoldt counting formula (*without* any truncations) for the number $N(E)$ of zeroes in the critical strip, with an imaginary part greater than 0 and less than or equal to E , was used to construct a saw potential comprised of an infinite number of branches. And this potential, in turn, generates explicitly the spectrum of energy levels associated to the solutions of the Schroedinger equation in each interval. The discrete energy spectrum will approach the zeta zeroes only in the *asymptotic* region (very large values of N). In this respect our construction is self-referential since the potential itself was constructed using the zeta zeroes.

Our potential is *fragmented*, “fractal”, in the sense that is comprised of infinite fragments obtained from an infinite number of tree-like branches. One finds also that there are cases when $x_m < x_n$ despite $m > n$, see figures (4-5). The location of these interval points, for example $x_8 < x_7$, appears to be “random”. Absence of evidence of order is not evidence of its absence. Random looking patterns may have hidden order. Ideally one would like to have other potentials. For example, related to the prime number distribution. However, the *exact* prime number counting function found by Riemann requires a knowledge of the zeta zeroes in the critical line, and once again one would end up with a self-referential construction. A potential based on the number counting function using the Riemann-Siegel Θ is another possibility worth exploring.

One could contemplate the possibility that the location of the nontrivial zeta zeroes in the critical line could behave as a quasicrystal array of atoms as postulated by [22],[34]. Instead of studying the bound states associated with our *aperiodic* saw potential, we may study the diffraction process from these atomic sites and see whether or not the patterns have sharp Bragg diffraction peaks as required in quasicrystals.

As described by Freeman Dyson and others [34], [35], a quasicrystal is a distribution of discrete point masses whose Fourier transform is a distribution of discrete point frequencies. Or to say it more briefly, a quasicrystal is a pure point distribution that has a pure point spectrum. Namely, it is an aperiodic but ordered (quasiperiodic) crystal, hence its name quasicrystal. This definition also includes as a special case the ordinary crystals, which are periodic distributions

with periodic spectra. Odlyzko [36] has published a computer calculation of the Fourier transform of the zeta-function zeroes. The calculation shows precisely the expected structure of the Fourier transform, with a sharp discontinuity at every logarithm of a prime or prime-power number and nowhere else. In other words, he showed that the distribution of the zeta zeros only appears random but is actually highly correlated to the distribution of primes by performing a Fourier transform.

There are some problems and questions raised in [35] that need to be addressed. For instance, if somehow one manages to get the classification of one-dimensional quasicrystals, we still have to face two huge issues : The classification will be an uncountable list of classes, each with uncountable elements. And given the many cases of models with the same diffraction, the classification is highly likely to be not nice. If we have a list of all quasicrystals, how do we check if the zeroes of the Riemann zeta function are or are not in the list, without knowing already all the zeroes?

Another issue raised in [35] is that the zeroes of zeta are not a Delone set, and this provides difficulty navigating the following issue: Let Λ be the set of zeroes. Let Λ' be the set obtained by moving all the zeroes, such that the n -th zero is moved by at most $1/n$. Then a diffraction pattern cannot differentiate between Λ and Λ' . Even if we were able to construct the Riemann quasicrystal associated with the nontrivial zeta zeros in the critical line this does not exclude the possibility of having zeroes off the critical line in case the RH fails.

The Fibonacci chain is the quintessential example of a one-dim quasicrystal. It is a one-dimensional aperiodic sequence which is a subset of the ring of Dirichlet integers $Z[\tau] = Z + Z\tau$, where τ is the Golden mean $\tau = (1 + \sqrt{5})/2$. The Fibonacci numbers are generated recursively by summing the previous two numbers. The tribonacci numbers are like the Fibonacci numbers, but instead of starting with two predetermined terms, the sequence starts with three predetermined terms and each term afterwards is the sum of the preceding three terms. The tetranacci numbers start with four predetermined terms, each term afterwards being the sum of the preceding four terms, and so forth. It is warranted to explore this possibility for the construction of a quasicrystal using chains based on generalized Fibonacci numbers [37].

Finally, we ought to explore the possibility that the one-dimensional quasicrystal might be obtained from the projection of a lattice in infinite dimensions, like the infinite simplex A_∞ , via the cut and projection mechanism involving irrational angles (irrational fraction of 2π). The irrational angles that generate the Dirichlet integers corresponding to the Fibonacci chains are the most physically interesting. One of us (KI) suggests that the special Dirichlet-integer-generating angles are a key to vastly narrowing the infinite universe of 1D quasicrystals that mathematicians are seeking for. The infinite simplex A_∞ is very relevant because the distribution of prime numbers correlates exactly with the distribution of prime simplexes, and prime A -lattices, within any bound as shown in [38], and where he introduced simplex-integers, as a form of geometric symbolism for numbers, such that the A_n lattice series (made of n -simplexes) corresponds logically to the integers. We shall leave this project for future work.

Table 1: Table of values of $E'_1(k)$ and M_k, N_k .

k	M_k	N_k	$E'_1(k)$
1	0.	1.	
2	-0.189471	0.858503	
3	-0.306782	0.733875	
4	-0.530412	0.770909	28.8823
5	-0.431255	0.569456	29.1688
6	-0.778562	0.706055	29.2093

Acknowledgements

One of us (CCP) thanks M. Bowers for assistance.

References

- [1] B. Riemann, On the number of prime numbers less than a given quantity, Monatsberichte der Berliner Akademie, November, 1859. (Translated by D. R. Wilkins, 1998).
- [2] A. A. Karatsuba, S. M. Voronin, *The Riemann zeta function*. [Translated from the Russian by Neal Koblitz] (Berlin-New York, Walter de Gruyter Pub., 1992); S. J. Patterson, *An introduction to the theory of the Riemann zeta function* (Cambridge, Univ. Press, 1988); H. M. Edwards, *Riemann's Zeta Function* (New York, Dover Pub., 2001); E. C. Titchmarsh, *The theory of the Riemann zeta-function* (Oxford, Clarendon Press, 1986).
- [3] S. Koolstra, "The Hilbert-Polya Conjecture", Bachelor Thesis, University of Amsterdam, 2013.
- [4] H. Wu and D. W. L. Sprung, *Phys. Rev. E* **48** (1993) 2595.
- [5] B. P. van Zyl and D. A. W. Hutchinson, *Phys. Rev. E* **67** (2003) 066211.
- [6] M. Berry and J. Keating, "The Riemann zeros and eigenvalue asymptotics", *SIAM Review*, **41**, no. 2 (1999) 236.
M. V. Berry and Z. V. Lewis, *Proc. Roy. Soc. Lond. A* **370** (1980) 459.
M. Berry, " H = xp and the Riemann zeros" in *Supersymmetry and Trace Formulae " Chaos and Disorder* , ed. J. Keating, D. Khmel'nitskii and I. Lerner, Kluwer 1999.
- [7] N. Katz and P. Sarnak, "Zeros of zeta functions and symmetry", *Bull. Amer. Math. Soc.* **36** (1999) 1.

- [8] R. Meyer, “A spectral interpretations for the zeros of the Riemann zeta function”, Mathematisches Institut, Georg-August-Universität Göttingen, Seminars Winter Term 2004/2005, 117-137., Universitätsdrucke Göttingen, Göttingen 2005.
- [9] B. S. Pavlov and L. D. Faddeev, “Scattering theory and automorphic functions” (Russian), Boundary value problems of mathematical physics and related questions in the theory of functions 6, Zap. Nauk. Sem. Leningrad. Otdel. Mat. Inst . Stekov (LOMI) **27** (1972) 161.
- [10] J. C. Lagarias, “Hilbert spaces of entire functions and Dirichlet L-functions”, in: Frontiers in Number Theory, Physics and Geometry I: On Random Matrices, Zeta Functions, and Dynamical Systems (P. E. Cartier, B. Julia, P. Moussa and P. van Hove, Eds.), Springer-Verlag: Berlin 2006, pp. 365-377.
- [11] A. Connes, “Trace formula in Noncommutative geometry and the zeros of the Riemann zeta function, *Selecta Math. (N. S.)* **5** (1999), 29.
- [12] L. de Branges, Self-reciprocal functions, *J. Math. Anal. Appl.* **9** (1964) 433.
L. de Branges, *Hilbert Spaces of Entire Functions*, (Prentice-Hall: Englewood Cliffs, NJ 1968).
- [13] A. Odlyzko, <http://www.dtc.umn.edu/odlyzko>.
- [14] J.F. Burnol, “Two complete and minimal systems associated with the zeros of the Riemann zeta function’, *J. Theor. Nombres Bordeaux* **16** (2004), 65.
- [15] J. Lagarias, “The Schroedinger Operator with Morse Potential on the Right Half Line” arXiv : 0712.3238.
- [16] M. Abramowitz and I. Stegun, *Handbook of Mathematical Functions* (Dover Publications, New York, 1970).
- [17] H. Buchholz, *The Confluent Hypergeometric Function* (Springer, New York, 1969).
- [18] E. W. Barnes, “On Functions defined by simple types of Hypergeometric Series” *Trans. Camb. Phil. Soc.* (xx, 1908).
- [19] E. T. Whittaker, G. N. Watson, *A Course of Modern Analysis* (Cambridge University Press, Cambridge, 1902).
- [20] M. Watkins, <http://empslocal.ex.ac.uk/people/staff/mrwatkin//>
- [21] P. M. Piravonu and K. Venkatesan, *A Textbook of Quantum Mechanics* (Tata-McGraw Hill Publishers, 1978).
C. Cohen-Tannoudji, B. Diu, and F. Laloe, *Quantum Mechanics* (Wiley Paperback 1996).

- [22] M. Lapidus, *In Search of the Riemann Zeros : Strings, Fractal Membranes and Noncommutative Spacetimes* American Mathematical Society, 2008.
M. Lapidus and M. van Frankenhuysen, *Fractal Geometry, Complex Dimensions and Zeta Functions: Geometry and Spectra of Fractal Strings* (Springer Monographs in Mathematics, 2013).
M. Lapidus and M. van Frankenhuysen, *Fractal geometry and number theory, fractal strings and zeros of the Zeta functions*, (Birkhauser, 2000).
- [23] G. Sierra, “The Riemann zeros as spectrum and the Riemann hypothesis” arXiv : 1601.01797.
G. Sierra and P. Townsend, ”Landau Levels and Riemann Zeros” arXiv : 0805.4079 [math-ph] .
G. Sierra, xp with interactions and the Riemann zeros, [arXiv: math-ph/0702034].
G. Sierra, *New Journal of Physics* **10** (2008) 033016.
- [24] A. LeClair, “Riemann Hypothesis and Random Walks: the Zeta case”, arXiv : 1601.00914.
G. Franca and A. LeClair, “A theory for the zeros of Riemann Zeta and other L-functions” areXiv : 1407.4358.
- [25] H. Montgomery, *Proc. Int. Congress of Mathematics* (Vancouver 1974, vol. 1, 379).
- [26] C. Castro, “On the Riemann Hypothesis, Area Quantization, Dirac Operators, Modularity and Renormalization Group” *International Journal of Geometric Methods in Modern Physics* **7**, No. 1 (2010) 1.
- [27] C. Castro, *International Journal of Geometric Methods in Modern Physics* **3**, no.2 (2006) 187.
- [28] C. Castro and J. Mahecha, “Fractal SUSY QM, Geometric Probability and the Riemann Hypothesis”, *International Journal of Geometric Methods in Modern Physics* **1** no.6 (2004) 751.
C. Castro and J. Mahecha, “Final steps towards a proof of the Riemann hypothesis”, [arXiv:hep-th/0208221].
- [29] M. Pitkanen, “A further step in the proof of Riemann hypothesis” arXiv : genmath/ 0109072.
- [30] P. Slater, A Numerical Examination of the Castro-Mahecha Supersymmetric Model of the Riemann Zeros, [arXiv: math.NT/0511188]; ” Fractal Fits to Riemann zeros”, *Canadian J. Physics* **85** (2007), 345 [arXiv: math-ph/0606005].
- [31] A. Karatsuba and M. Korolev, *Russian Math. Surveys* **60**, no. 3 (2005) 433.

- [32] R. Gorenflo and F. Mainardi, "Fractional Calculus : Integral and Differential Equations of Fractional Order" arXiv : 0805.3823.
- [33] A. Essin and D. Griffiths, "Quantum Mechanics of the $1/x^2$ potential" Am. J. Phys. **74** (2) (2006) 109.
- [34] F. Dyson, "Frogs and birds", Notices of the American Mathematical Society **56** (2009) 212.
- [35] J.Baez, "Quasicrystals and the Riemann Hypothesis"
https://golem.ph.utexas.edu/category/2013/06/quasicrystals_and_the_riemann.html
<http://mathoverflow.net/questions/133581/quasicrystals-and-the-riemann-hypothesis>
- [36] A. Oldlyzko, "Primes, quantum chaos and computers" , in *Number Theory : Proceedings of a Symposium* 4 May 1989, Washington, DC, USA (National Council, 1990), pp. 35-46
- [37] "Generalizations of Fibonacci numbers",
https://en.wikipedia.org/wiki/Generalizations_of_Fibonacci_numbers
- [38] K. Irwin, "Toward the Unification of Physics and Number Theory", QGR preprint, 2016.

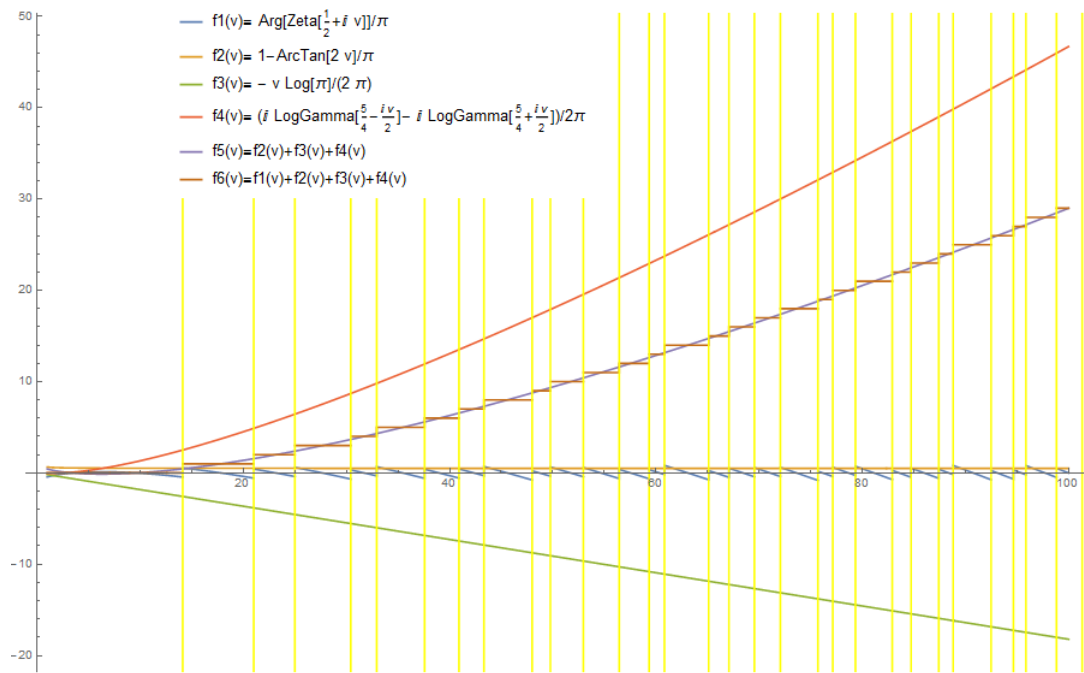


Figure 1: Number counting function

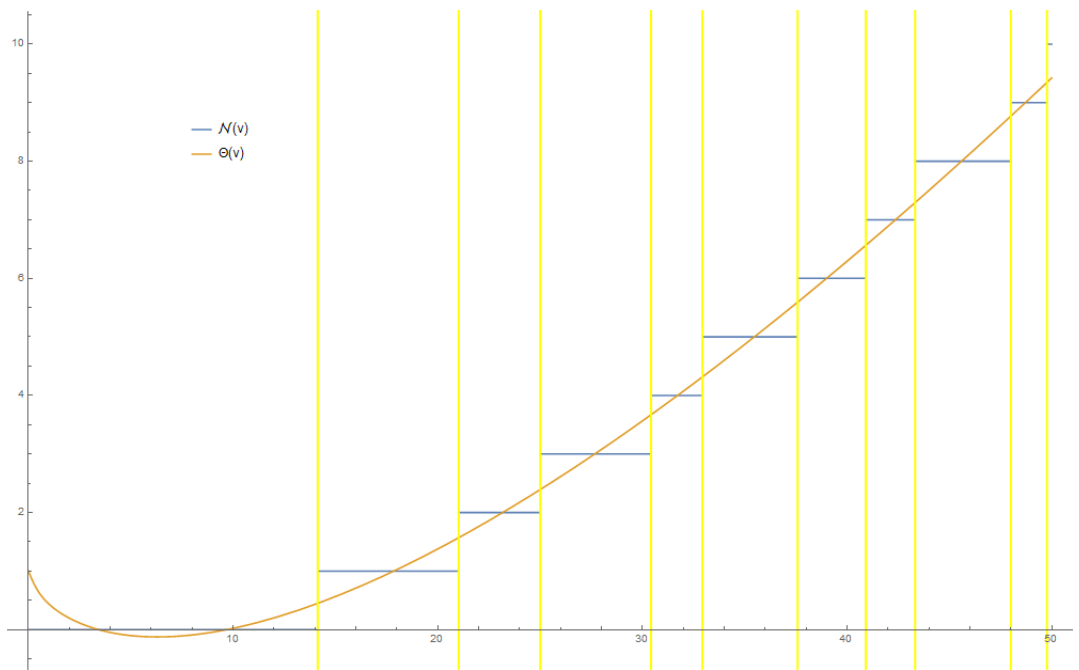


Figure 2: Number counting function using Riemann-Siegel Θ

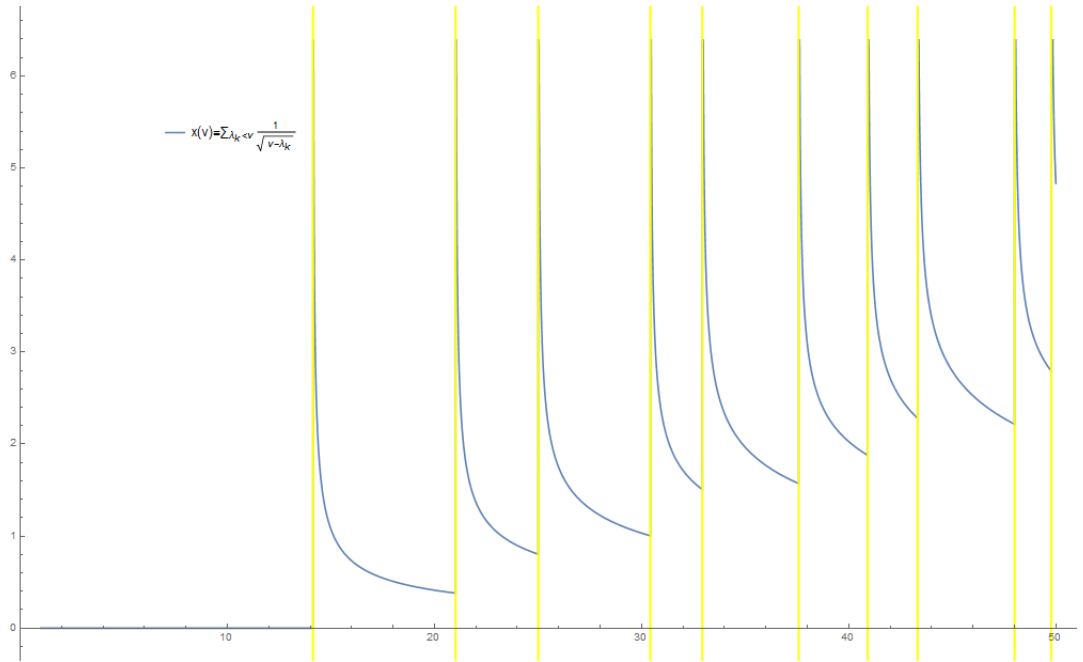


Figure 3: $x(V)$

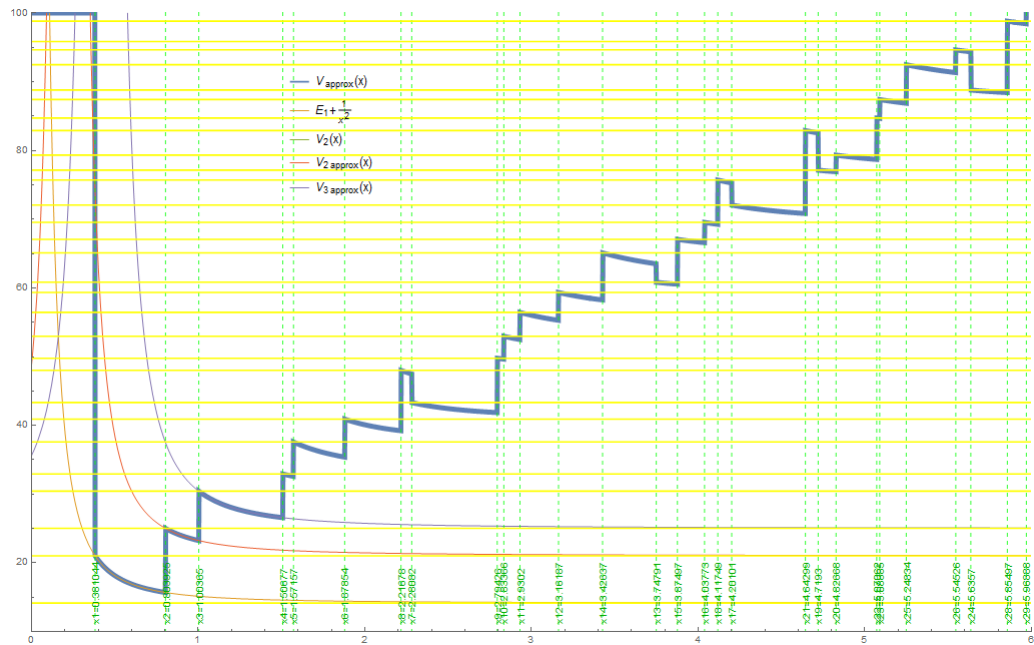


Figure 4: Approximate Potential $V(x)$ versus exact potential

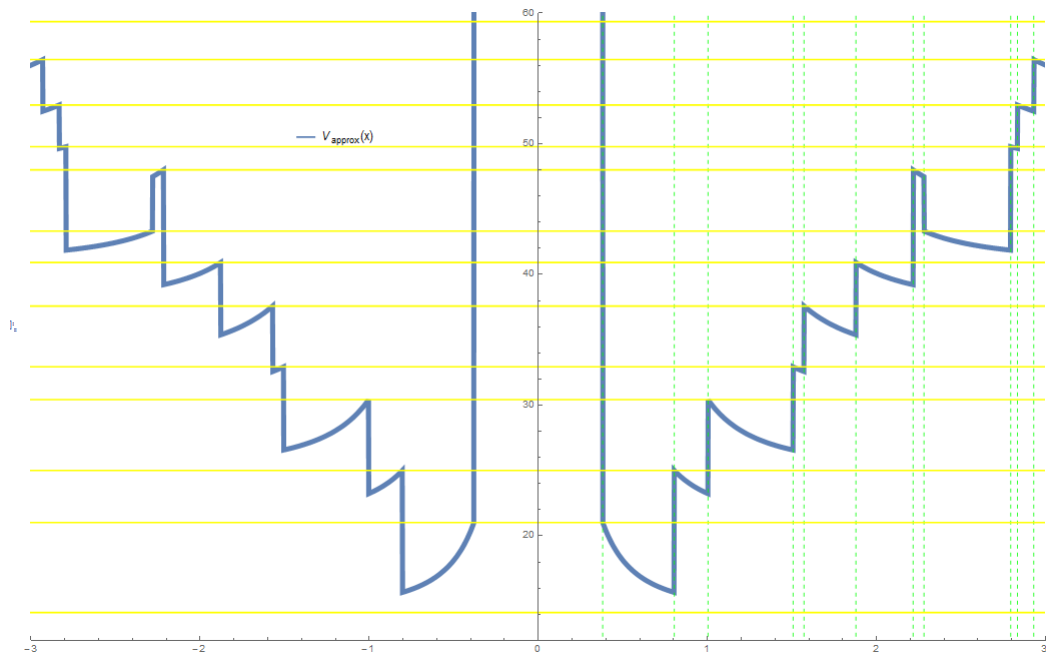


Figure 5: Symmetric approximate potential

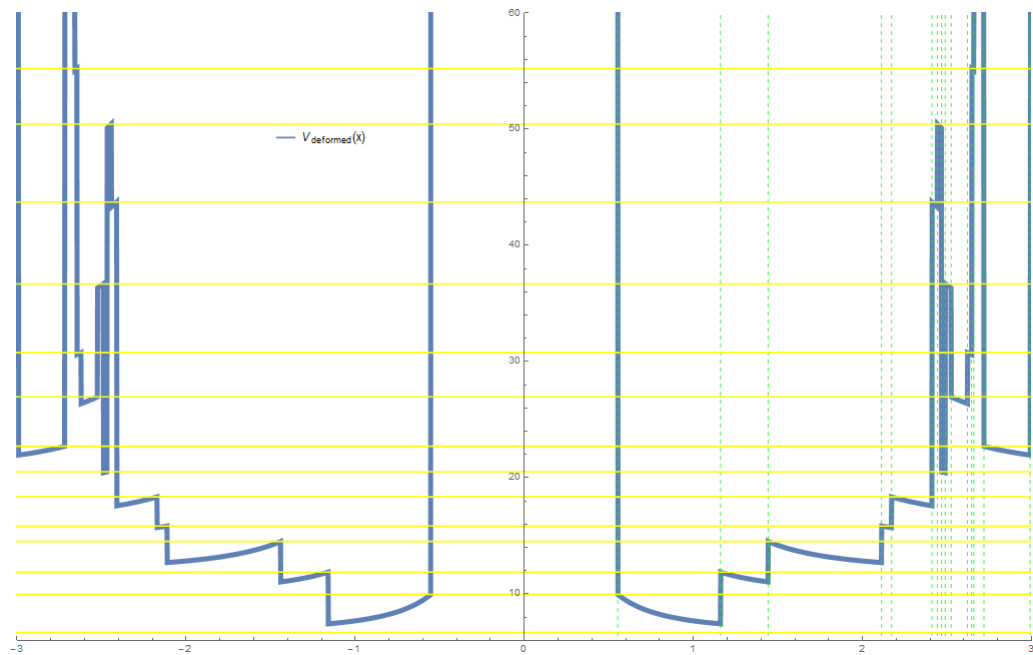


Figure 6: Fine-tuned potential

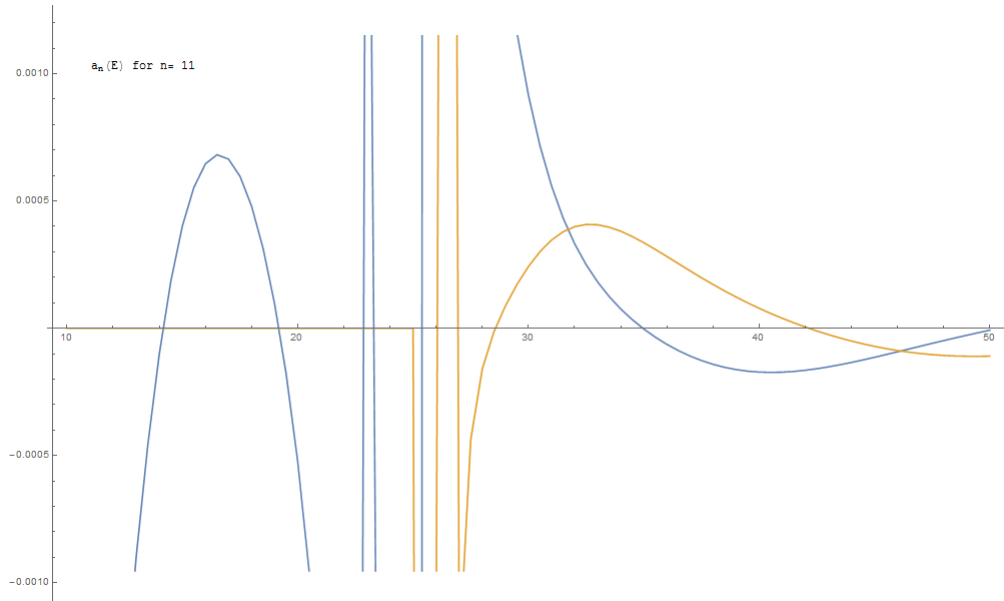


Figure 7: Characteristic function $a_{11}(E)$ for 11 intervals, when $\alpha = \beta$

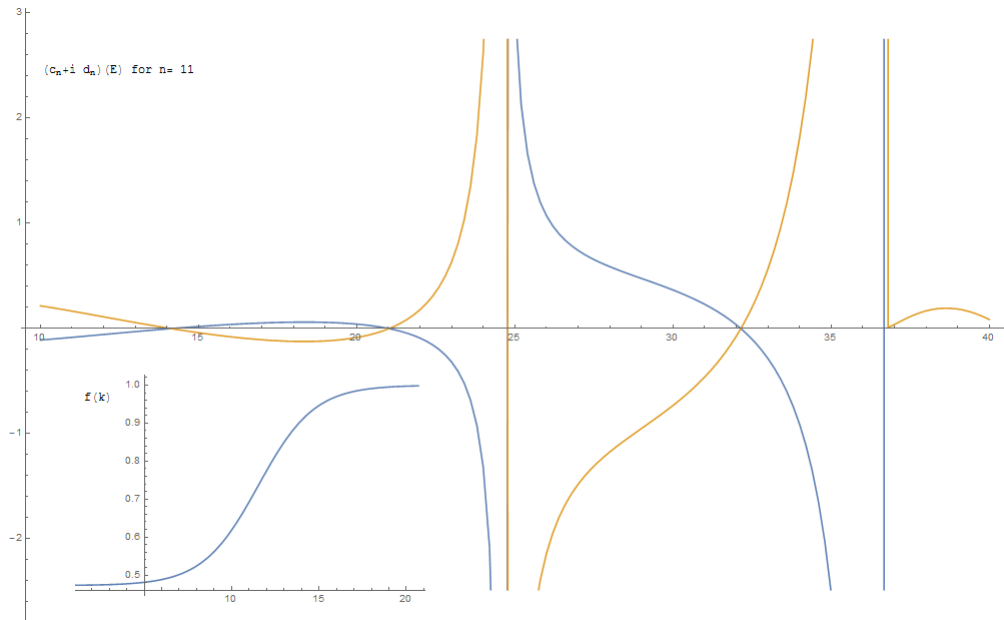


Figure 8: Characteristic function $(c_{11} + i d_{11})(E)$ for 11 intervals, when $\alpha = 665.142, \beta = 1407.11, \gamma = -0.628615$, inset of the fine-tuning logistic function $f(k)$

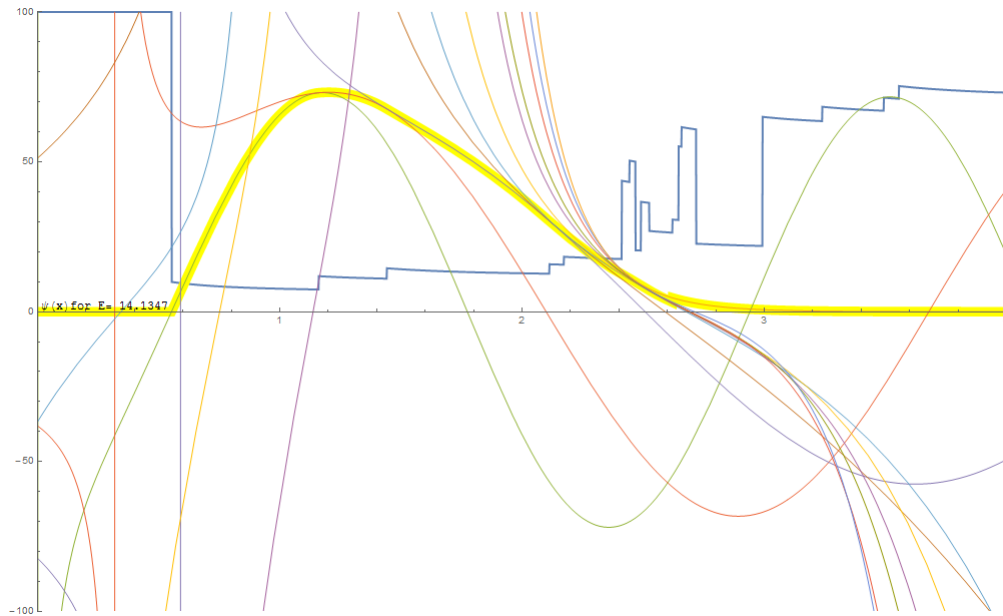


Figure 9: Wave function for 11 intervals for the eigenvalue $E_1(11) = 14.1347$ where $a_{1,E}$ has been scaled to 100 for convenience

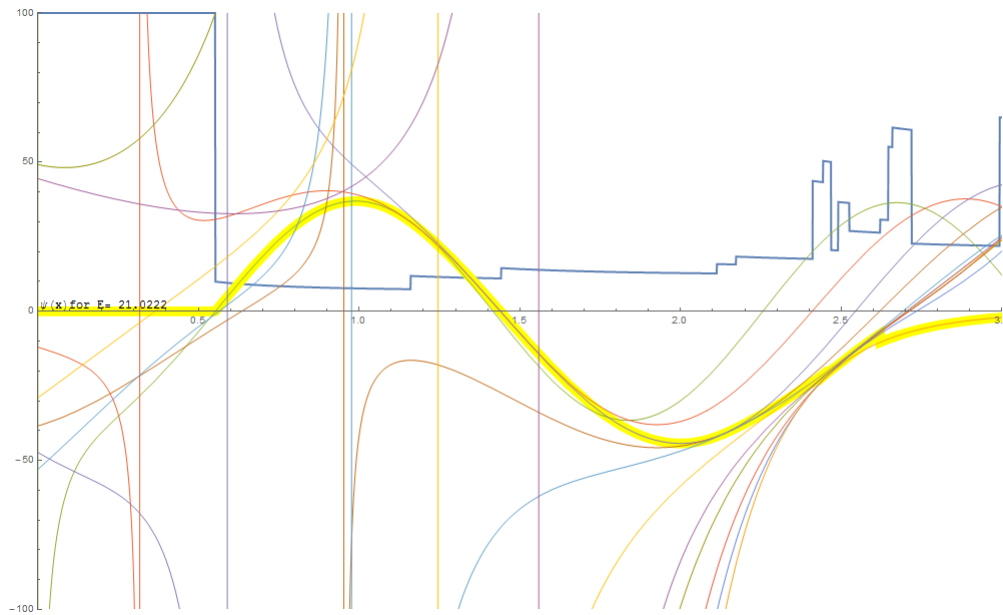


Figure 10: Wave function for 11 intervals for the eigenvalue $E_2(11) = 21.0222$ where $a_{1,E}$ has been scaled to 20 for convenience

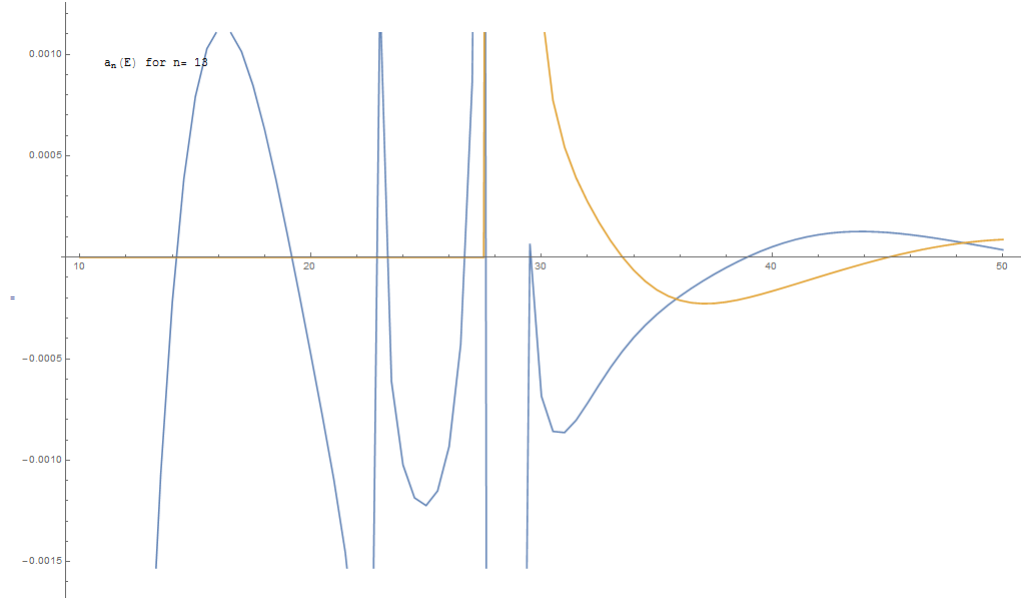


Figure 11: Characteristic function $a_{13}(E)$ for 13 intervals, when $\alpha = \beta$

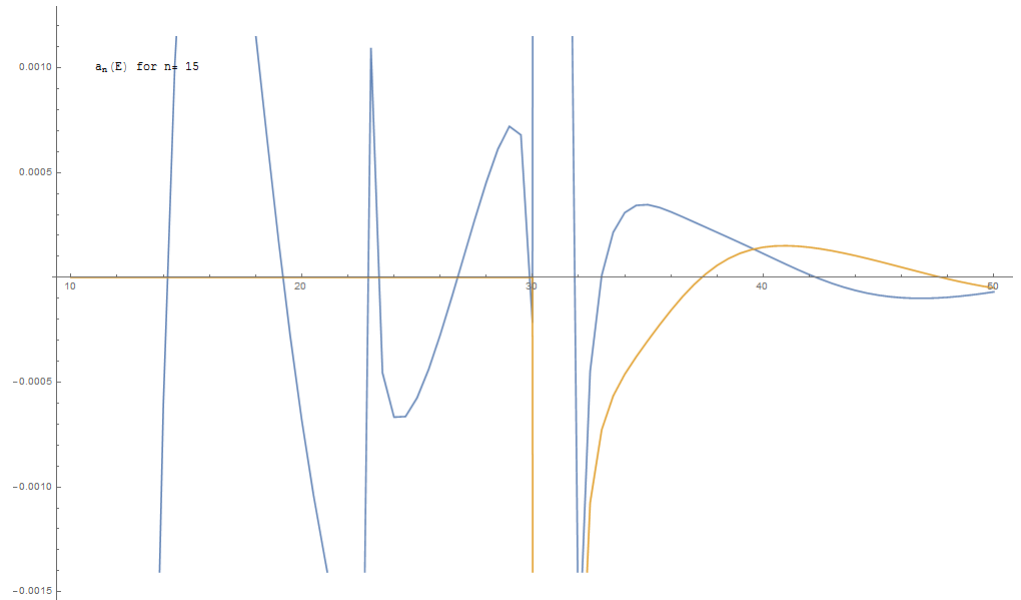


Figure 12: Characteristic function $a_{15}(E)$ for 15 intervals, when $\alpha = \beta$